

Article

Identification and Cloning of a Putative Male Fertility Gene Encoding an Oxidosqualene Cyclase in Qingke

Dian Lin ^{1,2}, Zhibin Xu ¹, Bo Feng ¹, Qiang Zhou ¹, Xiaoli Fan ^{1,*} and Tao Wang ^{1,3}

¹ Chengdu Institute of Biology, Chinese Academy of Sciences, Chengdu 610041, China; wangtao@cib.ac.cn (T.W.)

² University of Chinese Academy of Sciences, Beijing 101408, China

³ The Innovative Academy of Seed Design, Chinese Academy of Sciences, Beijing 100101, China

* Correspondence: fanxl@cib.ac.cn

Abstract: Anther development is crucial for controlling crop fertility. To elucidate the underlying mechanisms of reproductive development of highland barley (called Qingke in Chinese), two main Qingke cultivars, Zangqing 2000 and Ximala 22, were utilized. Transcriptome analysis showed that lipid, sugar and phenylpropane metabolisms might be the major pathways associated with Qingke male fertility by analyzing the possible common DEGs before anther maturation in both varieties. Additionally, 26 genes related to crop genic male sterility were screened to identify homologous genes for Qingke male sterile lines. Among them, *HORVU.MOREX.r3.7HG0634780 (HvtOSC12)*, an oxidosqualene cyclase, was highlighted as a candidate gene for affecting Qingke male fertility, as it is highly and especially expressed before Qingke anther maturation. Furthermore, *HvtOSC12* (including promoter sequence) was cloned by homology-based cloning. The further bioinformatic analysis deduced that MYBs might be one of the transcription factors affecting expression of *HvtOSC12* by responding to environmental changes. These results might lay a foundation for the potential applications for the creation of environment-sensitive genic male sterility in Qingke.

Keywords: anther development; environment-sensitive genic male sterility; triterpene pathway; *OSC12*



Citation: Lin, D.; Xu, Z.; Feng, B.; Zhou, Q.; Fan, X.; Wang, T.

Identification and Cloning of a Putative Male Fertility Gene Encoding an Oxidosqualene Cyclase in Qingke. *Agronomy* **2023**, *13*, 1292. <https://doi.org/10.3390/agronomy13051292>

Academic Editor: Andras Cseh

Received: 22 February 2023

Revised: 28 April 2023

Accepted: 28 April 2023

Published: 30 April 2023



Copyright: © 2023 by the authors. Licensee MDPI, Basel, Switzerland. This article is an open access article distributed under the terms and conditions of the Creative Commons Attribution (CC BY) license (<https://creativecommons.org/licenses/by/4.0/>).

1. Introduction

Highland barley (*Hordeum vulgare* L. var. *nudum* Hook. f.) is a type of hull-less barley, called “Qingke” in Chinese [1,2]. It usually shows strong cold resistance, resistance in barren soils, and wide adaptability. Thus, it is also the only cereal crop suitable for high altitudes, even 4200–4500 m sea level [3], such as the regions near the Himalayas (Nepal, Bhutan and Chinese Tibet) [4,5]. Therefore, for these people living in the highlands, it is the most important staple food and a major economic crop [6]. On the Qinghai–Tibet Plateau in China, Qingke has more than 3500 years of cultivation history [7]. As market demand rises, the sown area of Qingke has also gradually increased. According to the public report, the cultivation area of domestic Qingke had increased to 290,000 hectares in China, with yield reaching 4482.7 kg·ha⁻¹ and output value exceeding 5.2 billion CNY (Chinese yuan) in 2021. With its high content of protein, dietary fiber, vitamins, and particularly β-glucans, as well as other nutrients, Qingke continues to be studied [8]; its potentially positive anti-cancer, antilipidemic, and antiglycemic effects have been discovered and its demand continues to increase [9]. However, because of the high-altitude cultivation environment, the suitable planting and promotion area of Qingke is limited, and it is more dependent on the increase in yield per plant to ensure the overall production to meet the increasing market demand. Breeding for hybrid varieties by exploiting hybrid vigor is a helpful way to increase barley yields [10,11]. Therefore, breeding hybrid Qingke might further improve production capacity, which is also essential for developing the Qingke industry and regional food security.

Creating male sterile lines is a common and effective way to formulate hybrids in crop breeding, as it maintains hybrid vigor and improves crop yield potential [12,13]. Several crop genes involved in male fertility have been successively reported. For example, in wheat, Okada et al. [14] found that introducing biallelic frameshift mutations into a wheat male fertility gene, *Ms1*, resulted in complete male sterility in wheat cultivars Fielder and Gladius. Besides *Ms1*, several other male sterile lines, such as *Ms2*, *DEAP1* and *P450* male sterile lines have been generated for hybrid seed production in wheat, rice and sorghum [15–17]. Among these different sterile lines, the environment-sensitive genic male sterility (EGMS) lines, usually with mutated male fertility-related genes, make male gametes more sensitive to the environment during development and exhibit different fertility in the corresponding environments. This makes EGMS lines ideal for fertile control by taking advantage of natural environmental conditions to achieve self-fertilization in the fertile state or producing hybrid seeds in a sterile environment [18]. The common EGMS include temperature-sensitive male sterility (TMGS), photoperiod-sensitive male sterility (PGMS), and humidity-sensitive male sterility (HMGS), which have been used broadly in modern agriculture to formulate hybrids [19,20]. For instance, *HUMIDITY-SENSITIVE GENIC MALE STERILITY 1 (HMS1)*, encoding a β -ketoacyl-CoA synthase, has been reported to affect the biosynthesis of very-long-chain fatty acids and HGMS in rice [21]. Its mutants displayed decreased seed setting under low humidity but normal seed setting under high humidity, and thus developed HGMS lines with significant potential applications in hybrid rice breeding [21]. In addition, some environmentally influenced nuclear genes associated with male fertility have also been reported in wheat and rice [22–24]. One TGMS line, *tmsBS20T*, has been applied for hybrid wheat breeding in northern China [22]. Comparing wheat and rice with barley, progress in EGMS research has been much slower; only several related genes have been gradually discovered for EGMS, establishing favorable conditions for the creation of hybrid Qingke [25]. For example, *HvMS1*, encoding a PHD-finger transcription factor, was related to thermo-sensitive male sterility in barley, causing complete male sterility when overexpressed [26]. This helps to understand potential applications for environmentally switchable hybrid breeding systems [26]. As the application of and demand for Qingke gradually rose, more EGMS genes needed to be further identified.

One of the techniques and methodologies to understand the genes and mechanisms of anther development and male fertility in barley is to apply transcriptome analysis. [27,28]. However, only a few studies concentrated on the molecular mechanisms of reproductive development in Qingke [29]. In this study, we compared the transcriptional profiles of Qingke spikes at three developmental periods in two main cultivars, Zangqing 2000 and Ximala 22, to discover the possible common genes and mechanisms related to reproductive development and male fertility in different Qingke varieties, with the aim to create EGMS lines and improve production of hybrid Qingke.

2. Materials and Methods

2.1. Samples Selection and Preparation

Zangqing 2000 (ZQ2000) and Ximala 22 (XML22) were two Qingke varieties that were released in 2013 and 2009, respectively, in Tibet, China. Since they have excellent performance in yield and resistance, they both became representative varieties with large local cultivation areas. In this study, based on the performance of developing anthers, three spikes from the same period in both ZQ2000 and XML22 were separately mixed as one sample in three reproductive developmental stages around anther maturation for RNA-seq, referring to the Kirby and Appleyard's criteria [30]: (1) S1, the anther was white, i.e., before anther maturation; (2) S2, the anther was yellow and full, i.e., pollen just complete maturation but before anther dehiscence; (3) S3, the anther changed from yellow to white and dehisced, i.e., after completion of pollination. The seedlings of ZQ2000 were taken for cloning the complete sequence of the target gene, including the genomic sequence and the promoter sequence.

2.2. RNA Quantification and Qualification

RNA was extracted from spikes of each sample using TRIzol reagent, and the concentration and purity of RNA were measured using NanoDrop 2000 (Thermo Fisher Scientific, Wilmington, DE, USA). RNA integrity was assessed using the RNA Nano 6000 Assay Kit of the Agilent Bioanalyzer 2100 system (Agilent Technologies, Santa Clara, CA, USA), and all RNAs had the RIN value > 9, indicating that the RNA quality met the requirements for library construction.

2.3. RNA Isolation, Library Construction and RNA-Seq

The RNA sample preparations used a total of 1 µg RNA per sample as input material. Purification of mRNA from total RNA was performed using poly-T-oligo-attached magnetic beads. The NEBNext Ultra™ RNA Library Prep Kit for Illumina was used to create the sequencing libraries (NEB, Ipswich, MA, USA). In NEBNext First Strand Synthesis Reaction Buffer (5), fragmentation was carried out using divalent cations at elevated temperatures. A random hexamer primer and M-MuLV Reverse Transcriptase were used to create first-strand cDNA. DNA Polymerase I and RNase H were used to synthesize second-strand cDNA. Exonuclease/polymerase activities were used to convert the remaining overhangs into blunt ends. NEBNext Adaptor with hairpin loop structure was ligated after adenylation of 3' ends of DNA fragments to prepare for hybridization. The library fragments were purified with the AMPure XP system to select cDNA fragments preferentially of 240 bp length (Beckman Coulter, Beverly, MA, USA). Then, before PCR, 3 µL USER Enzyme (NEB, USA) was used with size-selected, adaptor-ligated cDNA at 37 °C for 15 min, followed by 5 min at 95 °C. To enrich the cDNA library, PCR amplification was carried out. Finally, PCR products were purified (AMPure XP system) and the quality of the library was evaluated using the Agilent Bioanalyzer 2100 system. The library preparations were sequenced and paired-end reads were generated on an Illumina platform.

2.4. Quality Control and Comparative Analysis

All further analyses depended on clean, high-quality data. Clean data (clean reads) were obtained in this step by removing adapter-containing reads, poly-N-containing reads, and low-quality reads from raw data. At the same time, the clean data's Q20, Q30, GC-content, and sequence duplication levels were calculated. Following that, the clean reads were mapped to the reference genome sequence by Hisat2 Tools soft [31]. Based on the reference genome, only reads with a perfect match or one mismatch were further analyzed and annotated.

2.5. Gene Functional Annotation

Gene function was annotated based on the following databases: NR (<https://www.ncbi.nlm.nih.gov/protein/>, accessed on 30 June 2022), Swiss-Prot (<http://www.uniprot.org/>, accessed on 30 June 2022), GO (<http://www.geneontology.org/>, accessed on 30 June 2022), COG (<http://www.ncbi.nlm.nih.gov/COG/>, accessed on 30 June 2022), KOG (<http://www.ncbi.nlm.nih.gov/KOG/>, accessed on 30 June 2022), Pfam (<http://pfam.xfam.org/>, accessed on 30 June 2022) and KEGG (<http://www.genome.jp/kegg/>, accessed on 30 June 2022).

2.6. Gene Expression Quantification

StringTie was used to assemble the aligned reads from each sample. The gene expression levels were determined by calculating FPKM values (fragments per kilobase of exon model per million mapped reads), which eliminated the effects of gene length and sequencing level on gene expression calculation [32].

2.7. Differentially Expressed Genes (DEGs)

Different expression analysis among different stages was performed with the DESeq package [33]. Criteria for differentially expressed genes were set as Fold Change (FC) ≥ 2

and False Discovery Rate (FDR) < 0.05. Venn analysis was used to analyze DEGs that have similar and unique trends between ZQ2000 and XML22.

2.8. Reverse Transcription and qRT-PCR Assays

The gene-specific primer pair was designed by Primer Premier 5.0 based on the target gene sequences, with Actin 3 [34] serving as the reference gene (Table S1). The RNA samples with a 260/280 ratio between 1.8 and 2.1 were transcribed into cDNA using the PrimeScript™ RT reagent Kit with gDNA Eraser (TaKaRa, Dalian, China). The relative expression of *OSC12* gene was performed on the QuantiStudio 3 Real-Time PCR System (Thermo Fisher, Waltham, MA, USA) using the TB Green® Premix Ex Taq™ II (TaKaRa, Dalian, China). Relative quantification was used to analyze data from real-time, quantitative PCR experiments [35]. To ensure reproducibility and reliability, each sample was analyzed in at least three independent biological replicates, with each biological replicate being run in triplicate for technical replicates. Statistical analyses were performed using the Data Processing System. $p < 0.05$ was considered significant, according to Tukey's test.

2.9. Primer Design and Cloning of Target Gene and Promoter

Taking the CDS of *OsOSC12* (XM_015795471) as the reference sequence, the homologous gene in Qingke was retrieved on the online database website (<http://202.194.139.32/blast/blast.html>, accessed on 5 July 2022). One homologous candidate gene was obtained from barley by sequence alignment, named *HotOSC12*.

The PCR amplification of *HotOSC12* in ZQ2000 was performed using Primer Premier 5.0 to design specific primers (Table S1). The primers were synthesized by Tsingke Biotechnology Co., Ltd., Beijing, China. The PCR amplification products were sequenced and spliced by BioEdit software (Figure S1).

The promoter clone was based on KAE8788986.1 sequence. Primer Premier 5.0 software was used for primer design, as shown in Table S1. After PCR amplification, the target fragments were recycled and purified. The TaKaRa T4 ligase kit was used for ligation and transformation. The positive clones were selected for identification and screening, then sent to Sangon Biotech (Shanghai, China) Co., Ltd. for sequencing. The sequencing results were blasted by BioEdit software.

2.10. Bioinformatics Analysis

Triticeae-Gene Tribe was used for homology searches (<http://wheat.cau.edu.cn/TGT/>, accessed on 12 July 2022). The open reading frames (ORFs) of sequences were analyzed by ORF finder (<https://www.ncbi.nlm.nih.gov/orffinder/>, accessed on 12 July 2022). ExpPASy-ProtParam was used to predict the physicochemical properties of protein (<https://web.expasy.org/protparam/>, accessed on 12 July 2022). The hydrophobicity was analyzed by ExpPASy-Scale (<https://web.expasy.org/protscale/>, accessed on 12 July 2022). TMHMM-2.0 was used to predict the transmembrane helices in proteins (<http://www.cbs.dtu.dk/services/TMHMM-2.0/>, accessed on 12 July 2022). PSORT II was used for subcellular localization (<https://web.expasy.org/protscale/>, accessed on 12 July 2022). NCBI Conserved Domains was used to predict the conserved domains (<https://www.ncbi.nlm.nih.gov/Structure/cdd/wrpsb.cgi>, accessed on 12 July 2022). Pfam was used to predict the functional domains (<http://pfam.xfam.org/search/sequence>, accessed on 12 July 2022). The protein secondary structures were predicted by PSIPRED (<http://bioinf.cs.ucl.ac.uk/psipred/>, accessed on 12 July 2022) and SOPMA (https://npsa-prabi.ibcp.fr/cgi-bin/npsa_automat.pl?page=npsa_sopma.html, accessed on 12 July 2022). The construct protein 3D structure was predicted by SWISS-MODEL (<https://swissmodel.expasy.org>, accessed on 12 July 2022) and Phyre2 (<http://www.sbg.bio.ic.ac.uk/phyre2/html/page.cgi?id=index>, accessed on 12 July 2022). STRING was used to predict protein interaction networks (<https://string-db.org/cgi/input>, accessed on 12 July 2022). NetPhos 3.1 was used to predict the phosphorylation site (www.cbs.dtu.dk/services/NetPhos, accessed on 12 July 2022). ClustalX2 software was used for homologous sequence comparison. MEGA11 software

(neighbor-joining method with 1000 tests) was used for phylogenetic tree construction. The promoter sequence cis-elements were analyzed by PlantCARE (<http://bioinformatics.psb.ugent.be/webtools/plantcare/html/>, accessed on 12 July 2022). BDGP was used to predict promoter transcription start sites (https://fruitfly.org/seq_tools/promoter.html, accessed on 12 July 2022).

3. Results

3.1. Transcriptome Sequencing Results

To study the characteristics of male reproductive development in Qingke, we used samples at three reproductive developmental stages with three replications in ZQ2000 and XML22, respectively, and a total of 18 libraries were constructed. After cleaning and quality checking, about 113.55 Gb total clean reads were obtained, and each library produced no less than 5.97 Gb clean reads. The GC contents of all samples were over 54.09%, and the percentage of Q30 bases was over 93.52%. Taking *Hordeum vulgare*.MorexV3.genome.fa as the reference genome for comparison, the comparison rate between each sample and the reference genome ranged from 91.01% to 94.43% (Table S2).

3.2. Functional Annotation

A total of 55,853 unigenes (80.90%) were annotated in at least one of the eight databases (Supplementary Materials S.1). The number and proportion of unigenes annotated in the eight databases were: COG (11,213, 16.2%), GO (35,414, 51.3%), KEGG (26,618, 38.6%), KOG (18,233, 26.4%), Pfam (32,223, 46.7%), Swiss-Prot (24,936, 36.1%), eggNog (35,942, 52.1%), NR (55,276, 80.1%). Among the 33,414 unigenes annotated in the Gene Ontology (GO) database, the “Intracellular” (27.3%) accounted for the greatest proportion of the cellular component (CC) category, the “Binding” (52.3%) and “Catalytic activity” (39.6%) were the most enrichment terms under the molecular function (MF) category, and the “Cellular process” (42.8%) and “Metabolic process” (38.1%) were the most enriched in the biological process (BP) category. The largest number of 1477 unigenes were enriched in the pathway of “Plant–pathogen interaction” (ko04626) among the 26,618 unigenes annotated to KEGG. The remaining unigenes were mainly concentrated in “Plant hormone signal transduction” (ko04075), “MAPK signaling pathway-plant” (ko04016) and “Oxidative phosphorylation” (ko00190). Out of the 25 KOG categories, the cluster for “General function prediction only” (23.2%) represented the largest group. The annotation of the NR database showed that the unigenes in the transcriptome were identical to sequences from *Hordeum vulgare* (71.8%), *Aegilops tauschii* (8.3%), *Triticum turgidum* (6.8%) and *Triticum aestivum* (3.9%), as expected.

3.3. Functional Annotation of DEGs and Enrichment Analysis

3.3.1. GO and KEGG Functional Enrichment Analysis of DEGs

Differentially expressed genes (DEGs) were identified in different stages of anther development (S1, S2 and S3) for ZQ2000 and XML22 using $|\log_2FC| \geq 1$ and false discovery rate (FDR) < 0.05 (Supplementary Materials S.1). In ZQ2000, for the comparisons of ZQ2000-S1 vs. ZQ2000-S2 and ZQ2000-S2 vs. ZQ2000-S3, 4868 DEGs (1905 up-regulated genes, 2963 down-regulated genes) and 4555 DEGs (2209 up-regulated genes, 2346 down-regulated genes) were identified, respectively. In XML22, for the comparisons of XML22-S1 vs. XML22-S2 and XML22-S2 vs. XML22-S3, 5499 DEGs (2646 up-regulated genes, 2853 down-regulated genes) and 5135 DEGs (2404 up-regulated genes, 2731 down-regulated genes) were identified, respectively (Figure S2).

Venn analysis revealed that 1282 up-regulated genes and 2046 down-regulated genes were observed to simultaneously exist in both ZQ2000-S1 vs. ZQ2000-S2 and XML22-S1 vs. XML22-S2 comparisons, indicating they might be the common genes involved in Qingke reproductive organ maturation despite different genetic backgrounds. However, fewer common DEGs (2275 DEGs), and fewer down-regulated genes especially (1213 down-regulated DEGs), were screened in these two comparisons of ZQ2000-S2 vs. ZQ2000-S3 and

XML22-S2 vs. XML22-S3, indicating that there are probably fewer of the same negatively regulatory genes ultimately affecting pollination (Figure 1, Supplementary Materials S.1).

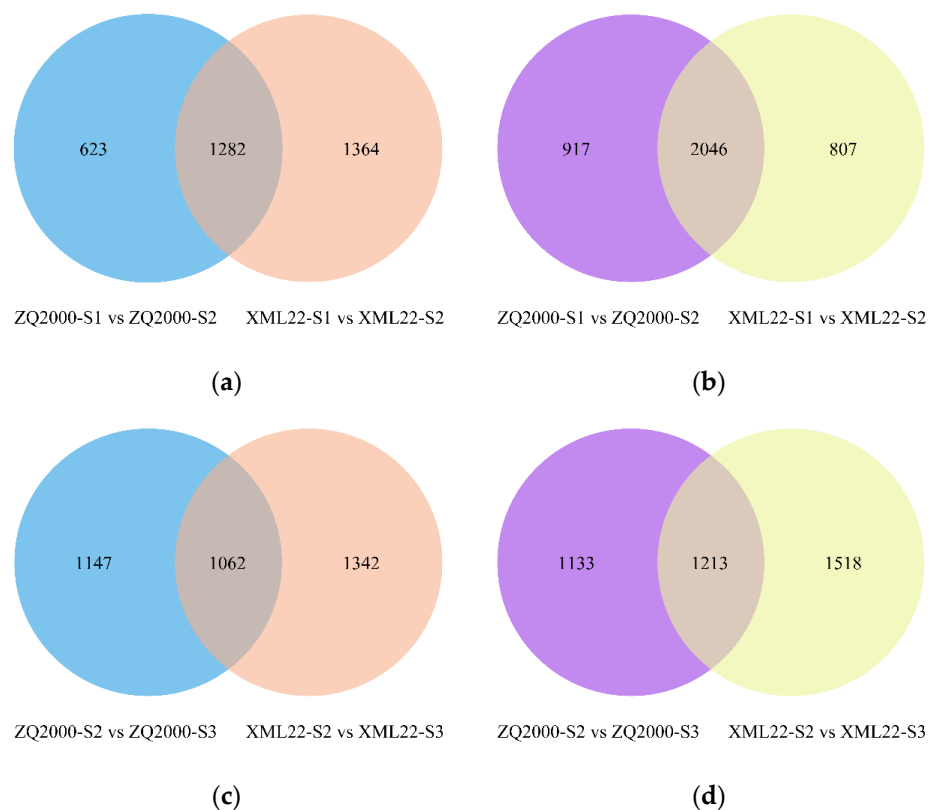


Figure 1. Venn diagram of up-regulated and down-regulated genes in comparisons. (a) Up-regulated genes for S1 vs. S2; (b) Down-regulated genes for S1 vs. S2; (c) Up-regulated genes for S2 vs. S3; (d) Down-regulated genes for S2 vs. S3. ZQ2000, Zangqing 2000; XML22, Ximala 22; S1, the anther was white, i.e., before anther maturation; S2, the anther was yellow and full, i.e., pollen at complete maturation but before anther dehiscence; S3, the anther changed from yellow to white and dehisced, i.e., after completion of pollination.

The GO annotations showed that the secondary classifications of common DEGs for S1 vs. S2 and S2 vs. S3 were similar (Supplementary Materials S.1). Under the classification of BP, the “Cellular process”, “Metabolic process” and “Single-organism process” were significantly enriched. While “Membrane”, “Cell” and “Cell part” were the most abundant categories in CC. Furthermore, under the MF classification, “Catalytic activity” and “Binding” were the most highly enriched GO terms (Figure S3).

The KEGG enrichment of these DEGs was also analyzed, and the top 20 pathways were shown in Figure S2 (Supplementary Materials S.1). Throughout anther development (S1 vs. S2 and S2 vs. S3), many DEGs (241 DEGs) were significantly enriched in sugar metabolism-related processes, such as “Starch and sucrose metabolism” (ko00500) and “Pentose and glucuronate interconversions” (ko00040). Meanwhile, the DEGs related to lipid metabolism were also mainly enriched, such as in the pathways of “Cutin, suberine and wax biosynthesis” (ko00073) and “Glycerophospholipid metabolism” (ko00564). In addition, the “Phenylpropanoid biosynthesis” (ko00940) and “Phenylalanine metabolism” (ko00360) were simultaneously significantly enriched. The results suggested that lipid metabolism, sugar metabolism and phenylpropanoid metabolism might also be important metabolic processes involved in the reproductive development process in Qingke, consistent with the other crops [36].

The formation of the pollen wall was a crucial step affecting male fertility in plants, mainly occurring before pollen maturation (S2 stage in this study) [37]. Further analy-

sis for the expressed change before anther complete maturation, i.e., S1 vs. S2, found that the common up-regulated DEGs in two varieties (Figure 2c) were concentrated only in the phenylpropane metabolisms, such as “Phenylalanine metabolism” (ko00360) and “Phenylpropanoid biosynthesis” (ko00940), while the common down-regulated DEGs (Figure 2e) were more comprehensively enriched in the three kinds of metabolisms mentioned above, such as “Pentose and glucuronate interconversions” (ko00040), “Starch and sucrose metabolism” (ko00500), “Glycerophospholipid metabolism” (ko00564) and “Fatty acid elongation” (ko00062), which have been found involved in reproductive development, indicating that these DEGs are maintained at a higher expression level before the S2 stage (at S1 stage) to affect male fertility by regulating the maturation of reproductive organs.

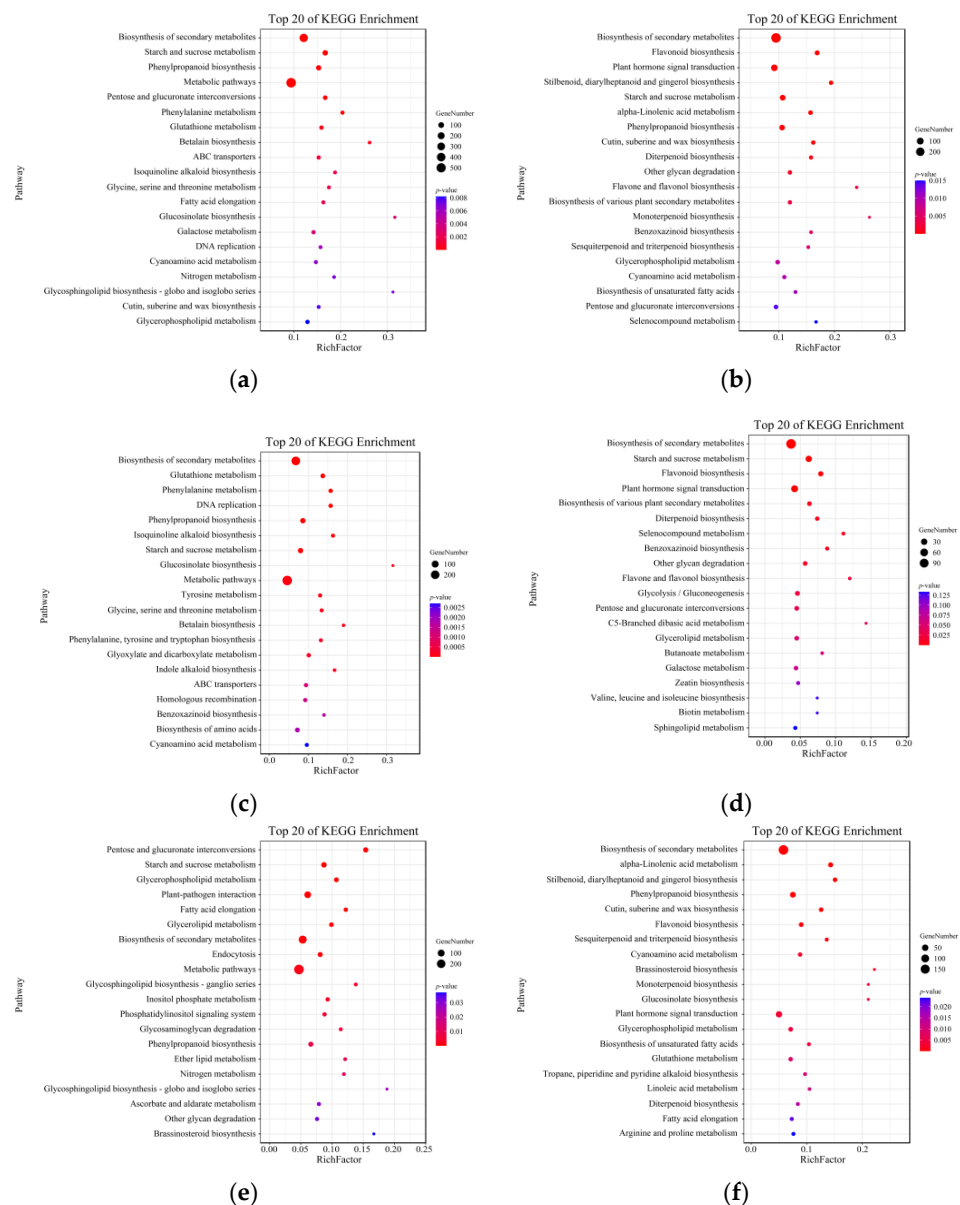


Figure 2. KEGG enrichment analysis of DEGs in this study. (a) All DEGs for S1 vs. S2; (b) All DEGs for S2 vs. S3; (c) Up-regulated DEGs for S1 vs. S2; (d) Up-regulated DEGs for S2 vs. S3; (e) Down-regulated DEGs for S1 vs. S2; (f) Down-regulated DEGs for S2 vs. S3. S1, the anther was white, i.e., before anther maturation; S2, the anther was yellow and full, i.e., pollen at complete maturation but before anther dehiscence; S3, the anther changed from yellow to white and dehisced, i.e., after completion of pollination.

3.3.2. Genes Related to Genic Male Sterility

In this study, 26 genic male sterility (GMS) genes were identified based on homologous genes in crops (Table 1). Most of these GMS genes showed different change trends in the ZQ2000 and XML22 (Supplementary Materials S.1), but only the homologous genes of *OsTMS18*, *OsOSC12* and *HMS1* exhibited consistent expression trends in Qingke during pollen maturation (S1 to S2), which is the most crucial period for determining male fertility. Moreover, only *HORVU.MOREX.r3.7HG0634780* for *OSC12* and *HORVU.MOREX.r3.1HG0027890* for *TDL1A* displayed consistent expression trends in both ZQ2000 and XML22 throughout the entire reproductive organ development stage (S1 to S3) (Figure S3a, Supplementary Materials S.1). The expression of *HORVU.MOREX.r3.1HG0027890* changed significantly only in the comparison of S2 vs. S3, indicating its affection mainly occurred after anther maturation. While *HORVU.MOREX.r3.7HG0634780*, the homologous gene of the well-known rice GMS gene *OsOSC12*, was significantly down-regulated in the S2 stage compared with S1, with the expectation that it was the important gene affecting male fertility. Meanwhile, the qRT-PCR analysis of *OSC12* gene revealed that its expression was significantly higher in the S1 stage compared to the S2 and S3 stages, thus confirming the accuracy of the RNA-seq (Figure 3b).

Table 1. The homologous genes of the genic male-sterility (GMS) genes in barley, rice and wheat.

No.	Gene Name	<i>Hordeum vulgare</i>	<i>Oryza sativa</i>	<i>Triticum aestivum</i>
1	<i>PMS1</i>	<i>HORVU.MOREX.r3.5HG0460900</i>	<i>Os11g0142500</i>	<i>TraesCS5A02G131300</i> <i>TraesCS5B02G133500</i> <i>TraesCS5D02G139800</i>
2	<i>OsTMS18</i>	<i>HORVU.MOREX.r3.1HG0051660</i>	<i>Os10g0524500</i>	<i>TraesCS1A02G187500</i> <i>TraesCS1B02G195300</i> <i>TraesCS1D02G189200</i>
3	<i>TMS5</i>	<i>HORVU.MOREX.r3.6HG0578870</i>	<i>Os02g0214300</i>	<i>TraesCS6A02G184600</i> <i>TraesCS6B02G211800</i> <i>TraesCS6D02G170400</i>
4	<i>TMS9-1</i>	<i>HORVU.MOREX.r3.5HG0485710</i>	<i>Os09g0449000</i>	<i>TraesCS5A02G233600</i> <i>TraesCS5B02G232100</i> <i>TraesCS5D02G240500</i>
5	<i>TMS2</i>	<i>HORVU.MOREX.r3.2HG0187560</i>	<i>Os07g0452500</i>	<i>TraesCS4A02G211000</i> <i>TraesCS2B02G420500</i> <i>TraesCS3D02G052200</i>
6	<i>OsPDCD5</i>	<i>HORVU.MOREX.r3.1HG0079230</i>	<i>Os05g0547850</i>	<i>TraesCS1A02G368100</i> <i>TraesCS1B02G387000</i> <i>TraesCS1D02G374000</i>
7	<i>CSA</i>	<i>HORVU.MOREX.r3.3HG0256690</i>	<i>Os01g0274800</i>	<i>TraesCS3A02G187800</i> <i>TraesCS3B02G217100</i> <i>TraesCS3D02G191400</i>
8	<i>OSMYOXIB</i>	<i>HORVU.MOREX.r3.6HG0629580</i>	<i>Os02g0816900</i>	<i>TraesCS6A02G390800</i> <i>TraesCS6B02G431400</i> <i>TraesCS6D02G377100</i>
9	<i>OsOSC12</i>	<i>HORVU.MOREX.r3.7HG0634780</i>	<i>Os08g0223900</i>	<i>TraesCS4A02G495100</i> <i>TraesCS7D02G004000</i> <i>TraesCSU02G191900</i>
10	<i>HMS1</i>	<i>HORVU.MOREX.r3.4HG0395960</i>	<i>Os03g0220100</i>	<i>TraesCS4A02G065300</i> <i>TraesCS4D02G242200</i> <i>TraesCS1B02G436300</i>
11	<i>OsHMS1I</i>	<i>HORVU.MOREX.r3.2HG0191470</i>	<i>Os04g0611200</i>	<i>TraesCS2A02G426000</i> <i>TraesCS2B02G446300</i> <i>TraesCS2D02G424100</i>

Table 1. Cont.

No.	Gene Name	<i>Hordeum vulgare</i>	<i>Oryza sativa</i>	<i>Triticum aestivum</i>
12	<i>OsTDF1</i>	HORVU.MOREX.r3.4HG0384200	Os03g0296000	TraesCS4A02G113000 TraesCS4B02G191200 TraesCS4D02G192400
13	<i>bHLH142</i>	HORVU.MOREX.r3.7HG0654120	Os05g0139100	TraesCS7A02G117100 TraesCS7B02G014500 TraesCS7D02G113100
14	<i>Udt1</i>	HORVU.MOREX.r3.2HG0136970	Os07g0549600	TraesCS2A02G212200 TraesCS2B02G237300 TraesCS2D02G218100
15	<i>Roc3</i>	HORVU.MOREX.r3.1HG0053250	Os10g0575600	TraesCS1A02G193400 TraesCS1B02G208400 TraesCS1D02G197300
16	<i>OsCrrl3</i>	HORVU.MOREX.r3.3HG0306540	Os05g0417000	TraesCS3A02G402300 TraesCS3B02G435700 TraesCS3D02G397200
17	<i>CYP704B2</i>	<i>Hordeum_vulgare_newGene_3892</i>	Os03g0168600	TraesCS4A02G019400 TraesCS4B02G284700 TraesCS4D02G283400
18	<i>OsGELP110</i>	HORVU.MOREX.r3.5HG0463140	Os11g0129500	TraesCS5A02G141800 TraesCS5B02G140600 TraesCS5D02G150300
19	<i>OsGPAT3</i>	HORVU.MOREX.r3.4HG0417370	Os12g0563000	TraesCS4A02G171600 TraesCSU02G250600 TraesCS4D02G143600
20	<i>SAP 62</i>	HORVU.MOREX.r3.4HG0390010	Os03g0263500	TraesCS4A02G088700 TraesCS4B02G215500 TraesCS4D02G216000
21	<i>CYP703A3</i>	HORVU.MOREX.r3.7HG0726310	Os08g0152400	TraesCS7A02G309300 TraesCS7B02G209300 TraesCS7D02G306000
22	<i>OsMS2</i>	HORVU.MOREX.r3.4HG0403060	Os03g0167600	TraesCS4A02G020500 TraesCS4B02G283200 TraesCS4D02G282000
23	<i>OsC4</i>	HORVU.MOREX.r3.7HG0686920	Os09g0525500	TraesCS7A02G269700 TraesCS7B02G167900 TraesCS7D02G270200
24	<i>sqv-2</i>	HORVU.MOREX.r3.3HG0298160	Os05g0427200	TraesCS3A02G389200 TraesCS3B02G419800 TraesCS3D02G380700
25	<i>OsGRX19</i>	HORVU.MOREX.r3.2HG0153120	Os07g0151100	TraesCS2A02G251700 TraesCS2B02G271600 TraesCS2D02G252500
26	<i>OsTDL1A</i>	HORVU.MOREX.r3.1HG0027890	Os12g0472500	TraesCS1A02G118900 TraesCS1B02G138400 TraesCS1D02G119800

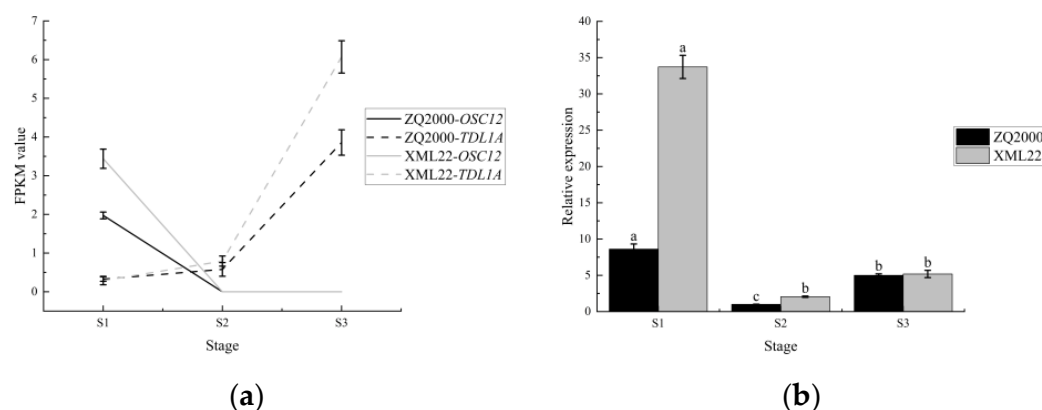


Figure 3. The expressed change of *OSC12* and *TDL1A* at different stages in ZQ2000 and XML22. (a) The FPKM value of *OSC12* and *TDL1A* at different stages; (b) The relative expression of *OSC12* at different stages. Different low case letters above columns indicate statistical differences at $p < 0.05$. ZQ2000, Zangqing 2000; XML22, Ximala 22; S1, the anther was white, i.e., before anther maturation; S2, the anther was yellow and full, i.e., pollen at complete maturation but before anther dehiscence; S3, the anther changed from yellow to white and dehisced, i.e., after completion of pollination.

The homologous genes of *HORVU.MOREX.r3.1HG0027890* in rice is *OsTDL1A/MIL2*, which binds to the leucine-rich repeat domain of MSP1 in order to limit sporocyte numbers [38]. *MIL2* regulates early anther cell differentiation and is responsible for the differentiation of primary parietal cells into secondary parietal cells in rice anthers, which in turn affects the male and female gametes' fertility [39]. Meanwhile, *multiple archesporial cells 1 (mac1)*, an ortholog of rice *TDL1A*, modulates cell proliferation and identity in early anther development in maize [40]. As for *OsOSC12*, its encoding enzyme (Oxidosqualene cyclase, OSC) catalyzed the cyclization of 2, 3-oxidosqualene into poaceatapelol, whose derivatives could affect pollen dehydration by reducing the accumulation of fatty acids in the pollen coat in rice [41]. Thus the mutants of *OsOSC12* were observed to the failure of pollen coat formation in rice, resulting in HGMS, which rendered the male plant sterile at low relative humidity ($RH < 60\%$), but fertile at high relative humidity ($RH > 80\%$) [41]. In addition, its homologous genes in maize, wheat and *Arabidopsis* have also been identified as the terpene cyclase, indicating it was functionally conserved across species [42,43].

To analyze the expression profiling of other related genes involved in the triterpene pathway for poaceatapelol synthesis, a total of 31 candidate structural genes encoding 16 triterpene metabolism-related enzymes were screened in this study (Table S3, Supplementary Materials S.1). Among these genes, only 15 were differentially expressed genes in either comparison (S1 vs. S2 or S2 vs. S3) (Table S3, Figures 4 and S4). Eight of these 15 ones showed differentially expressed in either ZQ2000 or XML22. Only seven DEGs, including *OSC12*, were commonly differentially expressed in both varieties (Figure 4).

3.4. Cloning of the Complete Sequence of Target Gene *HvtOSC12*

Since *OSC12* was highly conserved in several different species, it could be a candidate gene for GMS with potential applications. Therefore, *HvtOSC12* was cloned from ZQ2000 for subsequent study (Supplementary Materials S.2). The complete open reading frame (ORF) of *HvtOSC12* (Accession number: OM965356) was 2295 bp, encoding 764 amino acids. The structural analysis found that the gene consisted of 18 exons and 17 introns. Meanwhile, the transcriptional profiles showed that there were two alternative splicing events in *HvtOSC12*, including TSS (Alternative 5' first exon) and TTS (Alternative 3' last exon), which only predicted in S1 stage (Figure S5).

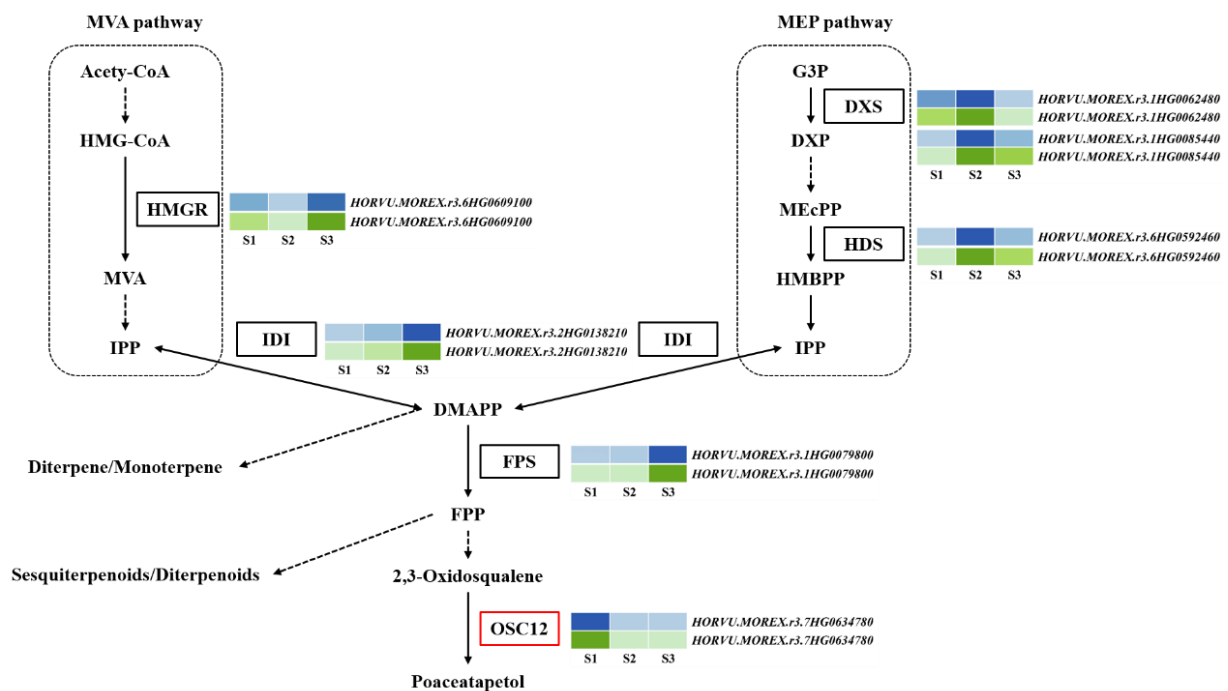


Figure 4. The expression profiles of Qingke DEGs encoding key enzymes involved in the possible poacetapetol biosynthesis pathway. The expression levels of genes in Zangqing 2000 and Ximala 22 are shown in blue and green, respectively. Both darker colors indicate the level according to the FPKM value. The box highlighted in red showed the candidate gene, *OSC12*. S1, the anther was white, i.e., before anther maturation; S2, the anther was yellow and full, i.e., pollen at complete maturation but before anther dehiscence; S3, the anther changed from yellow to white and dehiscence, i.e., after completion of pollination. MVA, Mevalonate; MEP, 2-C-methyl-D-erythritol-4-phosphate; HMG-CoA, 3-Hydroxy-3-methylglutaryl-CoA; IPP, Isopentenylpyrophosphate; G3P, Glyceraldehyde-3-phosphate; DXP, 1-Deoxy-D-xylulose-5-phosphate; MEcPP, 2-C-methyl-D-erythritol 2,4-cyclodiphosphate; HMBPP, 1-Hydroxy-2-methyl-2-(E)-butenyl 4-diphosphate; DMAPP, Dimethylallylpyrophosphate; FPP, Farnesyl diphosphate; HMGR, 3-Hydroxy-3-methylglutaryl-CoA reductase; DXS, 1-Deoxy-D-xylulose-5-phosphate synthase; HDS, (E)-4-hydroxy-3-methylbut-2-enyl-diphosphate synthase; IDI, Isopentenyl-diphosphate Delta-isomerase; FPS, Farnesyl diphosphate synthase; OSC, Oxidosqualene cyclase.

3.5. Bioinformatics Analysis of *HvtOSC12*

The predicted molecular weight of *HvtOSC12* protein was 86.45 kDa (Table S4). The 80th and 81st amino acids of *HvtOSC12* had the lowest score (−3.422); the 132ed amino acid had the highest score (2.578). *HvtOSC12* protein probably was a non-transmembrane hydrophilic (hydrophilic coefficient −0.316) protein located in the cytoplasm (74%).

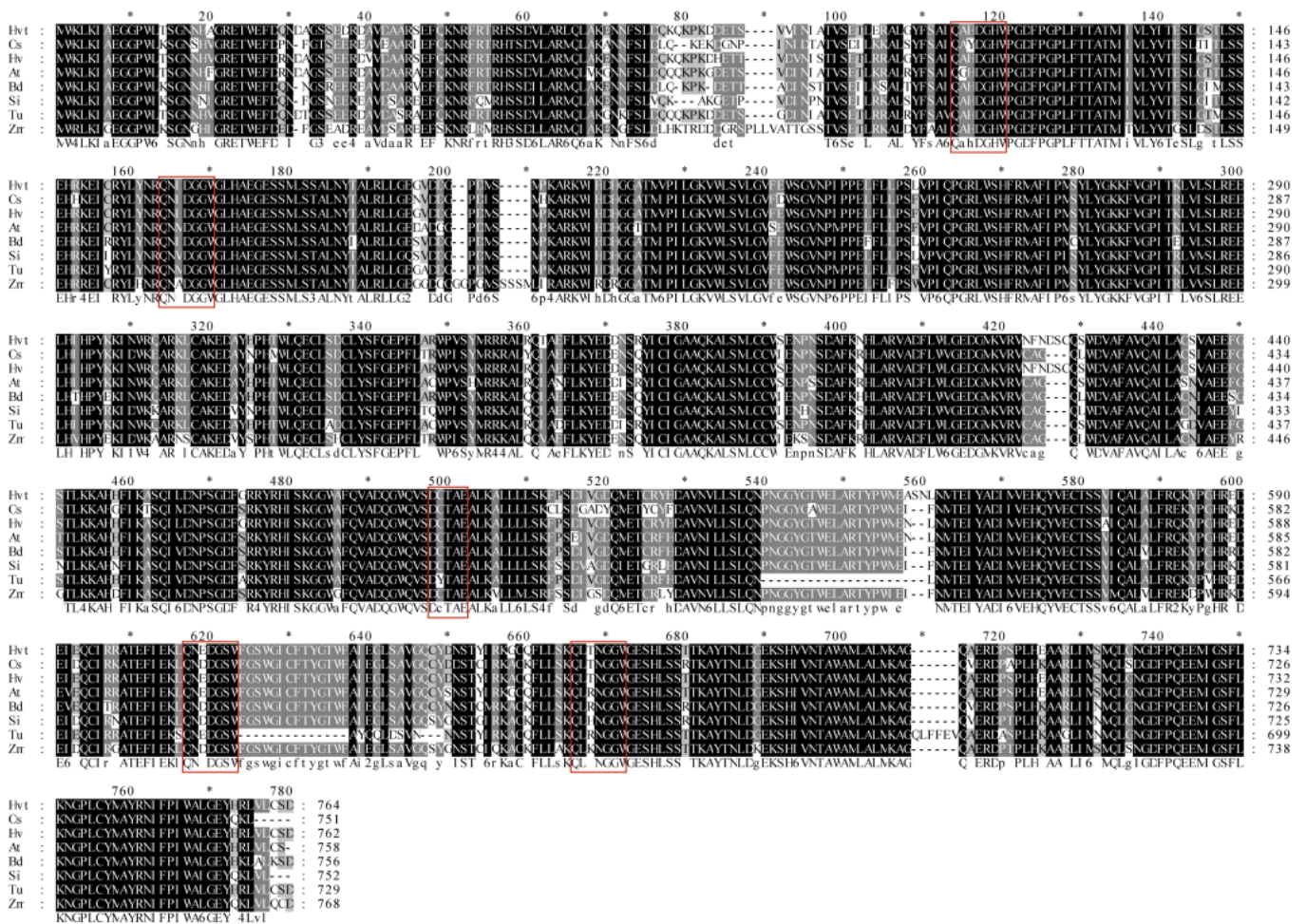
The conserved domain prediction showed SQCY_1 domain (amino acid positions 99–756) and PLN03012 superfamily domain (positions 1–760) existed. Additionally, the prediction indicated an SQHop_cyclase_N functional domain (positions 100–402) and an SQHop_cyclase_C functional domain (positions 421–757), which belong to the Six-hairpin glycosidase superfamily. The secondary structure showed that the proportion of α -helices was the largest in both predictions (Table S5). The three-dimensional structures were constructed with the “1w6j.1.A” (template consistency 42%) and “1w6kA” (template consistency 41%) as models, respectively (Figure S6).

The protein in the STRING database that most matched the *HvtOSC12* sequence was A0A287VBC0, belonging to the terpene cyclase/mutase family. It interacted with four proteins, including A0A287HSV6 (Flavodoxin-like domain-containing protein), M0Z560 (Uncharacterized protein), A0A287TCE0 (Peptidyl-prolyl cis-trans isomerase) and A0A287WGX1

(3-hydroxy-3-methylglutaryl coenzyme A reductase). The interaction associations were all textmining.

The prediction of cis-acting elements showed 29 kinds of 114 cis-acting elements in 2117 bp upstream of the 5' non-coding region of *HotOSC12*, including the core promoter element and enhancer element of typical eukaryotic promoters. In addition, it also included 11 action elements related to light response and four types of hormone response-related cis-elements (Table S6). As shown in Table S7, there were five potential transcription start sites with scores greater than 0.8. The accurate site of the *HotOSC12* promoter might be located in T at 692 bp upstream of ATG (Supplementary Materials S.3).

The results of homologous alignment showed that the sequence identity of Qingke and barley was 96.73%. Furthermore, all sequences have a highly conserved SQCY_1 domain (Figure 5a). The phylogenetic tree showed the *HotOSC12* in Qingke was most closely related to barley among the seven grass crops, while foxtail millet and maize were more distant (Figure 5b).



(a)

Figure 5. Cont.

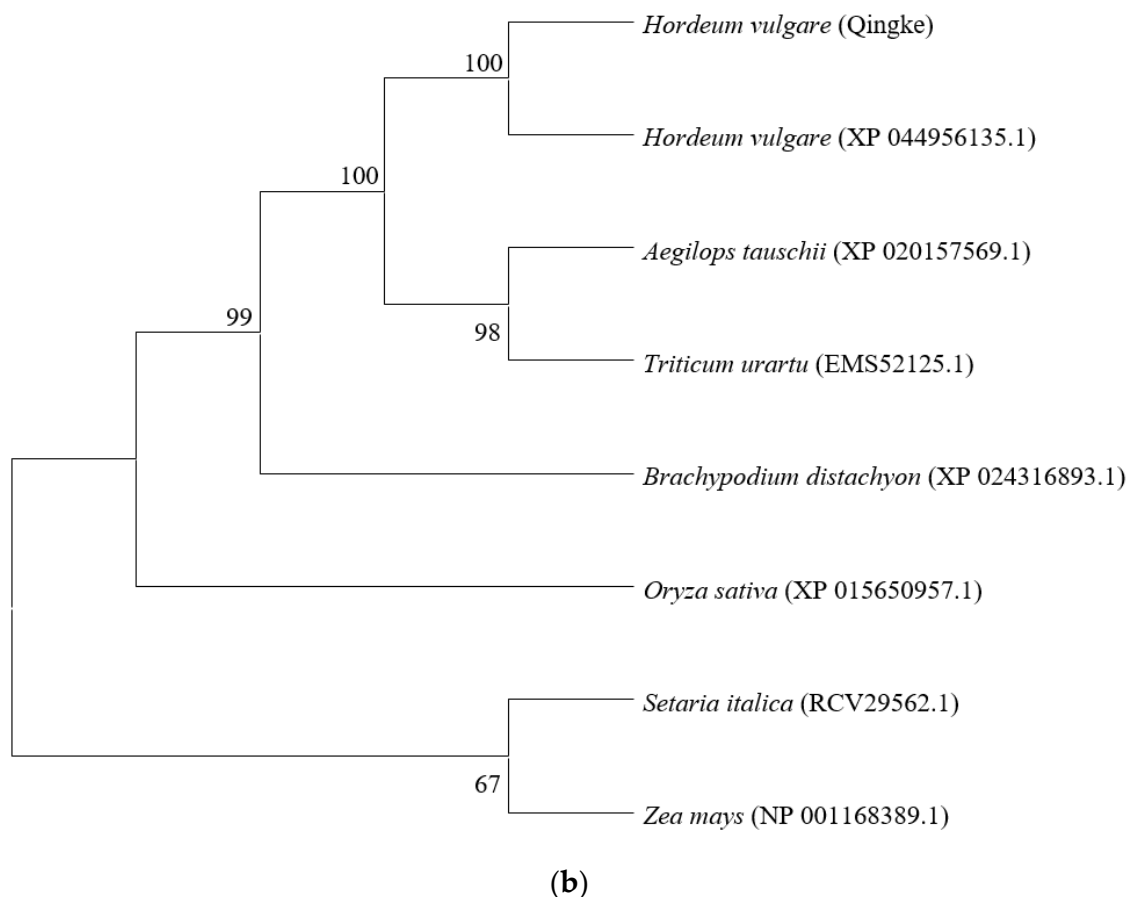


Figure 5. Analysis of the deduced amino acid sequences of *HvtOSC12* in Qingke with OSCs in other grass crops. (a) Multiple alignments of *HvtOSC12* and other grass crops. *, the marker line with 10 amino acids. (b) Phylogenetic tree constructed from the deduced amino acid sequences of *HvtOSC12* in Qingke and OSCs in other Gramineae plants. Hvt, *Hordeum vulgare* (Tibetan hull-less barley); Hv, *Hordeum vulgare*; Os, *Oryza sativa*; At, *Aegilops tauschii*; Bd, *Brachypodium distachyon*; Si, *Setaria italica*; Tu, *Triticum urartu*; Zm, *Zea mays*. The red box represents the DCTAE domain and the QW feature sequence.

4. Discussion

Cytoplasmic male sterility (CMS) and genic male sterility (GMS) are acknowledged as important genetic resources for heterosis utilization in crop production [12]. Compared with the traditional CMS-based three-line hybrid system, the two-line hybrid system uses an EGMS line that does not require a restorer line, thereby simplifying the hybrid process [44]. In recent years, P/TGMS lines have been used as the key materials in EGMS-based two-line systems for wheat and rice [13,45]. Given the importance of EGMS lines, it is valuable to research the mining of key genes and pathways of EGMS. The pollen wall has been focused in previous studies as it protects male gametophytes from various environmental stresses and microbial attacks during pollen development and also facilitates pollination [37]. Some reports revealed that GMS genes and pathways related to lipid and sugar metabolism control anther and pollen development, thus playing an essential role in male plant reproduction [46,47]. The expression of key genes for lipid, sugar, and phenylpropane accumulation was essential for forming male fertility in rice P/TGMS lines [36], and the “ABC transporters” pathway also regulated the lipid transport, which was crucial for forming both pollen walls and grains [48]. In this study, the common DEGs of both varieties for S1 vs. S2, which represented the anther developing and pollen layer formation process, were also primarily enriched in pathways of lipid, sugar and phenylpropane

metabolism, such as “Starch and sucrose metabolism” (ko00500), “Glycerophospholipid metabolism” (ko00564), “Fatty acid elongation” (ko00062) and “Pentose and glucuronate interconversions” (ko00040), consistent with the results of previous studies on the fertility of EGMS lines.

The temporal and spatial expression patterns of numerous genic male sterility (GMS) genes are highly conserved in grass crops [49]. In this study, 26 GMS genes (containing 11 EGMS) reported in rice, wheat and maize were used for homology searches. Since ZQ2000 and XML22 are both currently promoted cultivars in Tibet and have different genetic backgrounds, the discovery of genes that perform similarly among them may be more practical for studies on reproductive development in Qingke. Between the only two DEGs that showed consistent trends in ZQ2000 and XML22, significant changes in *HORVU.MOREX.r3.7HG0634780* (*OSC*) occurred during pollen maturation, the critical stage affecting male fertility. Kalaiyarasi and Vaidyanathan’s [50] results indicated that the pre- and post-meiotic genetic systems during anther development, and stamen and pistil primordial stages of panicle development, were sensitive to the expression of sterility. *CAMS1*, the homolog of *OSC* in *Arabidopsis*, encodes an oxidosqualene cyclase that generates predominantly monocyclic triterpene alcohol [42]. The *OsOSC12* has been identified as a triterpene synthase whose catalytic product is another triterpene alcohol, poaceatapelol [41]. The homologous genes of *OSC12* have similar functions, catalyzing the cyclization of oxysqualene into terpenoid alcohols, in different species. Poaceatapelol or its derivatives affect pollen dehydration by reducing the accumulation of fatty acids in the pollen coat, leading to a humidity-sensitive, sterile male phenotype in rice mutants [41].

In addition, the expression of key enzyme genes in the poaceatapelol synthesis pathway was analyzed (Table S3, Figure 4 and S4). These DEGs showed similar expression trends in both varieties, i.e., simultaneous up- or down-regulation of expression at one stage, suggesting that they performed more conservative functions and break through the limitations of different genetic backgrounds among the two varieties (Figure 4). Three DEGs involved in the mevalonate pathway (MVA), *HMGR* (*3-Hydroxy-3-methylglutaryl-CoA reductase*) and *IDI* (*Isopentenyl-diphosphate Delta-isomerase*), as well as the upstream gene for triterpene synthesis, *FPS* (*Farnesyl diphosphate synthase*), were up-regulated at the S3 stage when Qingke pollination was complete. Simultaneously, three DEGs mainly for the methylerythritol phosphate pathway (MEP) were up-regulated at the S2 stage when the anthers reached full maturity and were ready to start pollination in Qingke. These upstream DEGs might affect Qingke fertility by regulating other terpenoid syntheses after pollen maturation (Figure 4). Notably, *HvtOSC12*, the target gene responsible for poaceatapelol synthesis, was found to influence rice fertility by affecting pollen coat formation [41], and also showed high expression in Qingke at the S1 stage, the initial developmental period before anther maturation. This suggests that *HvtOSC12* might play a role in regulating anther maturation and influencing male fertility in Qingke, providing a possibility for the subsequent creation of Qingke male sterile lines.

The bioinformatics analysis showed that the homology of *HvtOSC12* and *OsOSC12* on amino acid sequence was up to 85.08%. The proportion of α -helices and the consistency of three-dimensional structures confirmed the stability of the *HvtOSC12* protein. The *SQCY_1* domain obtained by conserved domain prediction belongs to the ISOPREN_C2_like superfamily (PF00432), a member of the six-hairpin glycosidase superfamily, which confirmed the prediction of the functional domain. Conserved DCTAE sequences and a variable number of QW signature sequences were present in the amino acid sequences of most *OSCs*, which is consistent with the results of the comparison of graminaceous crops in this study. The former is related to substrate binding, while the latter is related to protein structural stability [51,52]. In addition, *OSC12* is conserved in grass crops based on evolutionary tree analysis.

The prediction of cis-acting elements in promoter sequences revealed that the *HvtOSC12* and *OsOSC12* genes shared similar promoter element types. The *HvtOSC12* promoter contained the stress response-related cis-element and the MYB binding sites, which

might collectively empower the *HvtOSC12* gene with the ability to adapt to environmental changes. The MYBs and several other transcription factors (TFs) were involved in plant triterpenoid biosyntheses in previous studies [53–55]. For instance, the *CiMYB42* transcription factor has been reported to regulate the expression of *CiOSC* by binding to the TTGTTG sequence (type II MYB core) of its promoter, further positively regulating limonoid biosynthesis, one of the triterpenoids [56]. In the *HvtOSC12* promoter sequences cloned in this study, the MBS core was also identified and might potentially bind an MYB transcription factor to regulate *HvtOSC12* mRNA transcription. Meanwhile, most of the differential expression of MYB/MYB-related transcription factor genes (22 genes) showed down-regulated trends in this study during S1 to S2, which occurred before the anther maturation (Table S8, Supplementary Materials S.4). It was consistent with the expression trend of *HvtOSC12*. Therefore, the MYBs might be one of the TFs affecting the expression of *HvtOSC12*, which may influence the poaceatapelol biosynthesis, anther development and ultimately regulate fertility in Qingke.

5. Conclusions

In this study, the spikes of ZQ2000 and XML22 with three reproductive developmental stages were subjected to transcriptome analysis, respectively. The lipid, sugar and phenylpropane metabolic pathways were found to be the main regulators of anther development in both cultivars. The candidate gene, *HORVU.MOREX.r3.7HG0634780* (*HvtOSC12*), was identified as a potential regulator of anther maturation and fertility in Qingke. *HvtOSC12* was subsequently cloned and analyzed by bioinformatics. It contains the typical domain of oxidosqualene cyclase with high conservation and might be sensitive to environmental changes based on the cis-acting element prediction of the promoter. Therefore, *HvtOSC12* was likely to play an important role in the reproductive development of Qingke, particularly in regulating male fertility by environment. Collectively, these results can be used for the creation of EGMS lines and provide insights into the anther development and fertility in Qingke.

Supplementary Materials: The following supporting information can be downloaded at: <https://www.mdpi.com/article/10.3390/agronomy13051292/s1>, Table S1: Primers of *HvtOSC12* gene for PCR amplification. Table S2: Statistics on mapping of sequencing data with the reference genome. ZQ2000, Zangqing 2000; XML22, Ximala 22; S1, the anther was white, i.e., before anther maturation; S2, the anther was yellow and full, i.e., pollen at complete maturation but before anther dehiscence; S3, the anther changed from yellow to white and dehisced, i.e., after completion of pollination. Table S3: Terpenoid biosynthesis-related gene annotation. The box highlighted in red and green showed the up-regulated and down-regulated trends, respectively. ZQ2000, Zangqing 2000; XML22, Ximala 22; S1, the anther was white, i.e., before anther maturation; S2, the anther was yellow and full, i.e., pollen at complete maturation but before anther dehiscence; S3, the anther changed from yellow to white and dehisced, i.e., after completion of pollination. Table S4: Physical and chemical properties of *HvtOSC12*. Table S5: Prediction of the secondary structure of *HvtOSC12* protein. Table S6: The cis-acting elements and functions of the *HvtOSC12* promoter. Table S7: Predictive analysis of the transcription start site for *HvtOSC12*. Table S8: The expression change trends of genes that encode MYB/MYB-related transcription factor. Figure S1: PCR amplification of DNA and promoter sequence of *HvtOSC12*. M, 200 bp DNA Ladder; 1, QK2000-1, the first DNA fragment of *HvtOSC12*; 2, QK2000-2, the second DNA fragment of *HvtOSC12*; 3, QK2000-3, the third DNA fragment of *HvtOSC12*; 4, Pro-1, the first promoter fragment of *HvtOSC12*; 5, Pro-2, the second promoter DNA fragment of *HvtOSC12*. Figure S2: Volcano plot analysis of DEGs in ZQ2000 and XML22 at different periods. (a) ZQ2000-S1 vs. ZQ2000-S2; (b) ZQ2000-S2 vs. ZQ2000-S3; (c) XML22-S1 vs. XML22-S2; (d) XML22-S2 vs. XML22-S3. ZQ2000, Zangqing 2000; XML22, Ximala 22; S1, the anther was white, i.e., before anther maturation; S2, the anther was yellow and full, i.e., pollen at complete maturation but before anther dehiscence; S3, the anther changed from yellow to white and dehisced, i.e., after completion of pollination. The spot highlighted in red and green showed the up-regulated and down-regulated trends, respectively. Figure S3: GO enrichment analysis of DEGs in Qingke at different stages. (a) S1 vs. S2; (b) S2 vs. S3. S1, the anther was white, i.e., before

anther maturation; S2, the anther was yellow and full, i.e., pollen at complete maturation but before anther dehiscence; S3, the anther changed from yellow to white and dehisced, i.e., after completion of pollination. Figure S4: The genes encoding key enzymes were involved in the possible poaceatpetol biosynthesis pathway. MVA, Mevalonate; MEP, 2-C-methyl-D-erythritol-4-phosphate; HMG-CoA, 3-Hydroxy-3-methylglutaryl-CoA; MAVP, Mvalonate-5-phosphate; MVAPP, Mvalonate-5-diphosphate; IPP, Isopentenylpyrophosphate; G3P, Glyceraldehyde-3-phosphate; DXP, 1-Deoxy-D-xylulose-5-phosphate; CDP-ME, 4-Diphosphocytidyl-2-C-methylerythritol; CDE-MEP, 4-Diphosphocytidyl-2-C-methyl-D-erythritol 2-phosphat; MEcPP, 2-C-methyl-D-erythritol 2,4-cyclodiphosphate; HMBPP, 1-Hydroxy-2-methyl-2-(E)-butenyl 4-diphosphate; DMAPP, Dimethylallylpyrophosphate; FPP, Farnesyl diphosphate; AACT, Acetyl-CoA C-acetyltransferase; HMGS, Hydroxymethylglutaryl-CoA synthase; HMGR, 3-Hydroxy-3-methylglutaryl-CoA reductase; MK, Mevalonate kinase; PMK, Phosphomevalonate kinase; MVD, Diphosphomevalonate decarboxylase; DXS, 1-Deoxy-D-xylulose-5-phosphate synthase; DXR, 1-Deoxy-Dlxylulose 5-phosphate reductoisomerases; MCT, 2-C-methyl-D-erythritol 4-phosphate cytidyltransferase; CMK, 4-Diphosphocytidyl-2-C-methyl-D-erythritol kinase; MCS, 2-C-methyl-D-erythritol 2,4-cyclodiphosphate synthase; HDS, (E)-4-hydroxy-3-methylbut-2-enyl-diphosphate synthase; HDR, (E)-4-hydroxy-3-methylbut-2-enyl-diphosphate reductase; IDI, Isopentenyl-diphosphate Delta-isomerase; FPS, Farnesyl diphosphate synthase; SQS, Squalene synthase; SQE, Squalene epoxidase; OSC, Oxidosqualene cyclase. Figure S5: The structure of *HvtOSC12*. The red and green boxes represented the alternative splicing events of TSS (Alternative 5' first exon) and TTS (Alternative 3' last exon) by prediction, respectively. Figure S6: Prediction of the tertiary structure of *HvtOSC12* protein. (a) Prediction by SWISS-MODEL; (b) Prediction by Phyre2. Supplementary Materials S.1. The Transcriptional Profile of All Unigenes. Supplementary Materials S.2. The Genomic Sequence of *HvtOSC12*. Supplementary Materials S.3. The Promoter Sequence of *HvtOSC12*. Supplementary Materials S.4. The Classification of Transcription Factors.

Author Contributions: Conceptualization, D.L. and X.F.; methodology, D.L., Z.X., B.F. and Q.Z.; software, D.L.; validation, D.L.; formal analysis, D.L.; data curation, D.L.; writing—original draft preparation, D.L.; writing—review and editing, D.L., X.F. and T.W.; funding acquisition, X.F. and T.W. All authors have read and agreed to the published version of the manuscript.

Funding: This research is supported by the Sichuan Science and Technology Program, China (2022ZDZX0016) and the Major Science and Technology Achievement Transformation of Central Universities and Institutes in Sichuan Projects, China (2022ZHCG0131).

Data Availability Statement: Data are contained within the article or Supplementary Materials.

Acknowledgments: We thank Biomarker Technologies Company (Beijing, China) for their high-throughput sequencing service and bioinformatic support.

Conflicts of Interest: The authors declare no conflict of interest.

References

- Hsu, T.W. Origin and phylogeny of cultivated barley with reference to the discovery of Ganze wild two-rowed barley *Hordeum spontaneum* C. koch. *Acta Genet. Sin.* **1975**, *2*, 6.
- Ma, D.Q.; Xu, T.W. The research on classification and origin of cultivated barley in Tibet Autonomous Region. *Sci. Agric. Sin.* **1988**, *21*, 7–14.
- Liu, Z.F.; Yao, Z.J.; Yu, C.; Zhong, Z.M. Assessing Crop Water Demand and Deficit for the Growth of Spring Highland Barley in Tibet, China. *J. Integr. Agric.* **2013**, *12*, 541–551. [[CrossRef](#)]
- Pandey, M.; Wagner, C.; Friedt, W.; Ordon, F. Genetic relatedness and population differentiation of Himalayan hullless barley (*Hordeum vulgare* L.) landraces inferred with SSRs. *Theor. Appl. Genet.* **2006**, *113*, 715–729. [[CrossRef](#)] [[PubMed](#)]
- Manjunatha, T.; Bisht, I.S.; Bhat, K.V.; Singh, B.P. Genetic Diversity in Barley (*Hordeum vulgare* L. ssp. *vulgare*) Landraces from Uttaranchal Himalaya of India. *Genet. Resour. Crop Evol.* **2007**, *54*, 55–65. [[CrossRef](#)]
- Zeng, X.Q.; Long, H.; Wang, Z.; Zhao, S.C.; Tang, Y.W.; Huang, Z.Y.; Wang, Y.L.; Xu, Q.J.; Mao, L.K.; Deng, G.B.; et al. The draft genome of Tibetan hullless barley reveals adaptive patterns to the high stressful Tibetan Plateau. *Proc. Natl. Acad. Sci. USA* **2015**, *112*, 1095–1100. [[CrossRef](#)]
- Zeng, X.Q.; Guo, Y.; Xu, Q.J.; Mascher, M.; Guo, G.G.; Li, S.C.; Mao, L.K.; Liu, Q.F.; Xia, Z.F.; Zhou, J.H.; et al. Origin and evolution of qingke barley in Tibet. *Nat. Commun.* **2018**, *9*, 5433. [[CrossRef](#)]
- Guo, T.L.; Horvath, C.; Chen, L.; Chen, J.; Zheng, B. Understanding the nutrient composition and nutritional functions of highland barley (Qingke): A review. *Trends Food Sci. Technol.* **2020**, *103*, 109–117. [[CrossRef](#)]

9. Lin, S.; Guo, H.; Lu, M.; Lu, M.Y.; Gong, J.D.B.; Wang, L.; Zhang, Q.; Qin, W.; Wu, D.T. Correlations of Molecular Weights of β -Glucans from Qingke (Tibetan Hulless Barley) to Their Multiple Bioactivities. *Molecules* **2018**, *23*, 1710. [[CrossRef](#)]
10. Mühleisen, J.; Maurer, H.P.; Stiewe, G.; Bury, P.; Reif, J.C. Hybrid Breeding in Barley. *Crop Sci.* **2013**, *53*, 819–824. [[CrossRef](#)]
11. Marulanda, J.J.; Mi, X.F.; Melchinger, A.E.; Xu, J.L.; Würschum, T.; Longin, C.F.H. Optimum breeding strategies using genomic selection for hybrid breeding in wheat, maize, rye, barley, rice and triticale. *Theor. Appl. Genet.* **2016**, *129*, 1901–1913. [[CrossRef](#)] [[PubMed](#)]
12. Kim, Y.J.; Zhang, D.B. Molecular Control of Male Fertility for Crop Hybrid Breeding. *Trends Plant Sci.* **2018**, *23*, 53–65. [[CrossRef](#)] [[PubMed](#)]
13. Yang, X.T.; Ye, J.L.; Niu, F.Q.; Feng, Y.; Song, X.Y. Identification and verification of genes related to pollen development and male sterility induced by high temperature in the thermo-sensitive genic male sterile wheat line. *Planta* **2021**, *253*, 83. [[CrossRef](#)] [[PubMed](#)]
14. Okada, A.; Arndell, T.; Borisjuk, N.; Sharma, N.; Watson-Haigh, N.S.; Tucker, E.J.; Baumann, U.; Langridge, P.; Whitford, R. CRISPR/Cas9-mediated knockout of *Ms1* enables the rapid generation of male-sterile hexaploid wheat lines for use in hybrid seed production. *Plant Biotechnol. J.* **2019**, *17*, 1905–1913. [[CrossRef](#)]
15. Liu, J.; Xia, C.; Dong, H.X.; Liu, P.; Yang, R.Z.; Zhang, L.C.; Liu, X.; Jia, J.Z.; Kong, X.Y.; Sun, J.Q. Wheat male-sterile 2 reduces ROS levels to inhibit anther development by deactivating ROS modulator 1. *Mol. Plant* **2022**, *15*, 1428–1439. [[CrossRef](#)]
16. Zhou, D.; Zou, T.; Zhang, K.X.; Xiong, P.P.; Zhou, F.X.; Chen, H.; Li, G.W.; Zheng, K.Y.; Han, Y.H.; Peng, K.; et al. *DEAP1* encodes a fasciclin-like arabinogalactan protein required for male fertility in rice. *J. Integr. Plant Biol.* **2022**, *64*, 1430–1447. [[CrossRef](#)]
17. Cigan, A.M.; Singh, M.; Benn, G.; Feigenbutz, L.; Kumar, M.; Cho, M.J.; Svitashv, S.; Young, J. Targeted mutagenesis of a conserved anther-expressed P450 gene confers male sterility in monocots. *Plant Biotechnol. J.* **2017**, *15*, 379–389. [[CrossRef](#)]
18. Ashraf, M.F.; Peng, G.Q.; Liu, Z.L.; Noman, A.; Alamri, S.; Hashem, M.; Qari, S.H.; Mahmoud Al Zoubi, O. Molecular Control and Application of Male Fertility for Two-Line Hybrid Rice Breeding. *Int. J. Mol. Sci.* **2020**, *21*, 7868. [[CrossRef](#)]
19. Bai, J.F.; Wang, Y.K.; Liu, Z.H.; Guo, H.Y.; Zhang, F.T.; Guo, L.P.; Yuan, S.H.; Duan, W.J.; Li, Y.M.; Tan, Z.G.; et al. Global survey of alternative splicing and gene modules associated with fertility regulation in a thermosensitive genic male sterile wheat. *J. Exp. Bot.* **2022**, *73*, 2157–2174. [[CrossRef](#)]
20. Yu, B.; Liu, L.T.; Wang, T. Deficiency of very long chain alkanes biosynthesis causes humidity-sensitive male sterility via affecting pollen adhesion and hydration in rice. *Plant Cell Environ.* **2019**, *42*, 3340–3354. [[CrossRef](#)]
21. Chen, H.Q.; Zhang, Z.G.; Ni, E.D.; Lin, J.W.; Peng, G.Q.; Huang, J.L.; Zhu, L.Y.; Deng, L.; Yang, F.F.; Luo, Q.; et al. HMS1 interacts with HMSII to regulate very-long-chain fatty acid biosynthesis and the humidity-sensitive genic male sterility in rice (*Oryza sativa*). *New Phytol.* **2020**, *225*, 2077–2093. [[CrossRef](#)] [[PubMed](#)]
22. Ru, Z.G.; Zhang, L.P.; Hu, T.Z.; Liu, H.Y.; Yang, Q.K.; Weng, M.L.; Wang, B.; Zhao, C.P. Genetic analysis and chromosome mapping of a thermo-sensitive genic male sterile gene in wheat. *Euphytica* **2015**, *201*, 321–327. [[CrossRef](#)]
23. Zhou, H.; Zhou, M.; Yang, Y.Z.; Li, J.; Zhu, L.Y.; Jiang, D.G.; Dong, J.F.; Liu, Q.J.; Gu, L.F.; Zhou, L.Y.; et al. RNase Z^{S1} processes *Ubl40* mRNAs and controls thermosensitive genic male sterility in rice. *Nat. Commun.* **2014**, *5*, 4884. [[CrossRef](#)] [[PubMed](#)]
24. Singh, M.; Albertsen, M.C.; Cigan, A.M. Male Fertility Genes in Bread Wheat (*Triticum aestivum* L.) and Their Utilization for Hybrid Seed Production. *Int. J. Mol. Sci.* **2021**, *22*, 8157. [[CrossRef](#)]
25. Fernández-Gómez, J.; Wilson, Z.A. A barley PHD finger transcription factor that confers male sterility by affecting tapetal development. *Plant Biotechnol. J.* **2014**, *12*, 765–777. [[CrossRef](#)]
26. Fernández-Gómez, J.; Talle, B.; Wilson, Z.A. Increased expression of the *MALE STERILITY1* transcription factor gene results in temperature-sensitive male sterility in barley. *J. Exp. Bot.* **2020**, *71*, 6328–6339. [[CrossRef](#)]
27. Muñoz-Amatriain, M.; Svensson, J.T.; Castillo, A.M.; Cistué, L.; Close, T.J.; Vallés, M.P. Transcriptome analysis of barley anthers: Effect of mannitol treatment on microspore embryogenesis. *Physiol. Plant* **2006**, *127*, 551–560. [[CrossRef](#)]
28. Liu, H.R.; Li, G.; Yang, X.J.; Kuijjer, H.N.J.; Liang, W.Q.; Zhang, D.B. Transcriptome profiling reveals phase-specific gene expression in the developing barley inflorescence. *Crop J.* **2020**, *8*, 71–86. [[CrossRef](#)]
29. Shi, T.; Dimitrov, I.; Zhang, Y.L.; Tax, F.E.; Yi, J.; Gou, X.P.; Li, J. Accelerated rates of protein evolution in barley grain and pistil biased genes might be legacy of domestication. *Plant Mol. Biol.* **2015**, *89*, 253–261. [[CrossRef](#)]
30. Kirby, E.J.M.; Appleyard, M. *Wheat Breeding*; Chapman and Hall: London, UK, 1987; pp. 287–311.
31. Kim, D.; Langmead, B.; Salzberg, S.L. HISAT: A fast spliced aligner with low memory requirements. *Nat. Methods* **2015**, *12*, 357–360. [[CrossRef](#)]
32. Perteu, M.; Perteu, G.M.; Antonescu, C.M.; Chang, T.C.; Mendell, J.T.; Salzberg, S.L. StringTie enables improved reconstruction of a transcriptome from RNA-seq reads. *Nat. Biotechnol.* **2015**, *33*, 290–295. [[CrossRef](#)] [[PubMed](#)]
33. Love, M.I.; Huber, W.; Anders, S. Moderated estimation of fold change and dispersion for RNA-seq data with DESeq2. *Genome Biol.* **2014**, *15*, 550. [[CrossRef](#)] [[PubMed](#)]
34. Xu, C.; Zhan, C.; Huang, S.; Xu, Q.; Tang, T.; Wang, Y.; Luo, J.; Zeng, X. Resistance to Powdery Mildew in Qingke Involves the Accumulation of Aromatic Phenolamides Through Jasmonate-Mediated Activation of Defense-Related Genes. *Front. Plant Sci.* **2022**, *13*, 900345. [[CrossRef](#)] [[PubMed](#)]
35. Livak, K.J.; Schmittgen, T.D. Analysis of relative gene expression data using real-time quantitative PCR and the 2(-Delta Delta C(T)) Method. *Methods* **2001**, *25*, 402–408. [[CrossRef](#)]

36. Sun, Y.J.; Fu, M.; Ang, Y.; Zhu, L.; Wei, L.N.; He, Y.; Zeng, H.L. Combined analysis of transcriptome and metabolome reveals that sugar, lipid, and phenylpropane metabolism are essential for male fertility in temperature-induced male sterile rice. *Front. Plant Sci.* **2022**, *13*, 945105. [[CrossRef](#)] [[PubMed](#)]
37. Jiang, J.; Zhang, Z.; Cao, J. Pollen wall development: The associated enzymes and metabolic pathways. *Plant Biol.* **2013**, *15*, 249–263. [[CrossRef](#)] [[PubMed](#)]
38. Zhao, X.; De Palma, J.; Oane, R.; Gamuyao, R.; Luo, M.; Chaudhury, A.; Hervé, P.; Xue, Q.; Bennett, J. OsTDL1A binds to the LRR domain of rice receptor kinase MSP1, and is required to limit sporocyte numbers. *Plant J.* **2008**, *54*, 375–387. [[CrossRef](#)]
39. Hong, L.L.; Tang, D.; Shen, Y.; Hu, Q.; Wang, K.J.; Li, M.; Lu, T.G.; Cheng, Z.K. MIL2 (MICROSPORELESS2) regulates early cell differentiation in the rice anther. *New Phytol.* **2012**, *196*, 402–413. [[CrossRef](#)]
40. Wang, C.J.R.; Nan, G.L.; Kelliher, T.; Timofejeva, L.; Vernoud, V.; Golubovskaya, I.N.; Harper, L.; Egger, R.; Walbot, V.; Cande, W.Z. Maize *multiple archesporial cells 1 (mac1)*, an ortholog of rice *TDL1A*, modulates cell proliferation and identity in early anther development. *Development* **2012**, *139*, 2594–2603. [[CrossRef](#)]
41. Xue, Z.Y.; Xu, X.; Zhou, Y.; Wang, X.N.; Zhang, Y.C.; Liu, D.; Zhao, B.B.; Duan, L.X.; Qi, X.Q. Deficiency of a triterpene pathway results in humidity-sensitive genic male sterility in rice. *Nat. Commun.* **2018**, *9*, 604. [[CrossRef](#)]
42. Kolesnikova, M.D.; Wilson, W.K.; Lynch, D.A.; Obermeyer, A.C.; Matsuda, S.P.T. *Arabidopsis* camelliol C synthase evolved from enzymes that make pentacycles. *Org. Lett.* **2007**, *9*, 5223–5226. [[CrossRef](#)] [[PubMed](#)]
43. Guo, C.F.; Xiong, X.C.; Dong, H.; Qi, X.Q. Genome-wide investigation and transcriptional profiling of the oxidosqualene cyclase (OSC) genes in wheat (*Triticum aestivum*). *J. Syst. Evol.* **2022**, *60*, 1378–1392. [[CrossRef](#)]
44. Virmani, S.S.; Ilyas-Ahmed, M. Environment-sensitive genic male sterility (EGMS) in crops. *Adv. Agron.* **2001**, *72*, 139–195. [[CrossRef](#)]
45. Wu, L.Y.; Jing, X.H.; Zhang, B.L.; Chen, S.J.; Xu, R.; Duan, P.G.; Zou, D.N.; Huang, S.J.; Zhou, T.B.; An, C.C.; et al. A natural allele of *OsMS1* responds to temperature changes and confers thermosensitive genic male sterility. *Nat. Commun.* **2022**, *13*, 2055. [[CrossRef](#)] [[PubMed](#)]
46. Liu, S.S.; Li, Z.W.; Wu, S.W.; Wan, X.Y. The essential roles of sugar metabolism for pollen development and male fertility in plants. *Crop J.* **2021**, *9*, 1278–1290. [[CrossRef](#)]
47. Wan, X.Y.; Wu, S.W.; Li, Z.W.; An, X.L.; Tian, Y.H. Lipid Metabolism: Critical Roles in Male Fertility and Other Aspects of Reproductive Development in Plants. *Mol. Plant* **2020**, *13*, 955–983. [[CrossRef](#)] [[PubMed](#)]
48. Kretzschmar, T.; Burla, B.; Lee, Y.; Martinoia, E.; Nagy, R. Functions of ABC transporters in plants. *Essays Biochem.* **2011**, *50*, 145–160. [[CrossRef](#)]
49. Wan, X.Y.; Wu, S.W.; Li, Z.W.; Dong, Z.Y.; An, X.L.; Ma, B.; Tian, Y.H.; Li, J.P. Maize Genic Male-Sterility Genes and Their Applications in Hybrid Breeding: Progress and Perspectives. *Mol. Plant* **2019**, *12*, 321–342. [[CrossRef](#)]
50. Kalaiyarasi, R.; Vaidyanathan, P. Cytological screening of rice TGMS lines. *Plant Breed.* **2003**, *122*, 334–338. [[CrossRef](#)]
51. Abe, I.; Prestwich, G.D. Molecular cloning, characterization, and functional expression of rat oxidosqualene cyclase cDNA. *Proc. Natl. Acad. Sci. USA* **1995**, *92*, 9274–9278. [[CrossRef](#)]
52. Poralla, K.; Hewelt, A.; Prestwich, G.D.; Abe, I.; Reipen, I.; Sprenger, G. A specific amino acid repeat in squalene and oxidosqualene cyclases. *Trends Biochem. Sci.* **1994**, *19*, 157–158. [[CrossRef](#)] [[PubMed](#)]
53. Mertens, J.; Pollier, J.; Vanden-Bossche, R.; Lopez-Vidriero, I.; Franco-Zorrilla, J.M.; Goossens, A. The bHLH Transcription Factors TSAR1 and TSAR2 Regulate Triterpene Saponin Biosynthesis in *Medicago truncatula*. *Plant Physiol.* **2016**, *170*, 194–210. [[CrossRef](#)]
54. Singh, A.K.; Kumar, S.R.; Dwivedi, V.; Rai, A.; Pal, S.; Shasany, A.K.; Nagegowda, D.A. A WRKY transcription factor from *Withania somnifera* regulates triterpenoid withanolide accumulation and biotic stress tolerance through modulation of phytosterol and defense pathways. *New Phytol.* **2017**, *215*, 1115–1131. [[CrossRef](#)] [[PubMed](#)]
55. Liu, T.; Luo, T.; Guo, X.Q.; Zou, X.; Zhou, D.H.; Afrin, S.; Li, G.; Zhang, Y.; Zhang, R.; Luo, Z.Y. PgMYB2, a MeJA-Responsive Transcription Factor, Positively Regulates the Dammareniol Synthase Gene Expression in *Panax Ginseng*. *Int. J. Mol. Sci.* **2019**, *20*, 2219. [[CrossRef](#)] [[PubMed](#)]
56. Zhang, P.; Liu, X.F.; Yu, X.; Wang, F.S.; Long, J.H.; Shen, W.X.; Jiang, D.; Zhao, X.C. The MYB transcription factor *CiMYB42* regulates limonoids biosynthesis in citrus. *BMC Plant Biol.* **2020**, *20*, 254. [[CrossRef](#)] [[PubMed](#)]

Disclaimer/Publisher’s Note: The statements, opinions and data contained in all publications are solely those of the individual author(s) and contributor(s) and not of MDPI and/or the editor(s). MDPI and/or the editor(s) disclaim responsibility for any injury to people or property resulting from any ideas, methods, instructions or products referred to in the content.